



Received 12 October 2021  
Accepted 21 December 2021

Edited by V. Jancik, Universidad Nacional Autónoma de México, México

**Keywords:** 4-[(benzylamino)carbonyl]-1-methylpyridinium; molecular structure; crystal structure; Hirshfeld surface analysis.

**CCDC references:** 2130345; 2130344

**Supporting information:** this article has supporting information at journals.iucr.org/e

## 4-[(Benzylamino)carbonyl]-1-methylpyridinium halogenide salts: X-ray diffraction study and Hirshfeld surface analysis

Svitlana V. Shishkina,<sup>a,b\*</sup> Anna M. Shaposhnik,<sup>a</sup> Vyacheslav M. Baumer,<sup>a</sup> Vitalii V. Rudiuk<sup>c</sup> and Igor A. Levandovskiy<sup>d</sup>

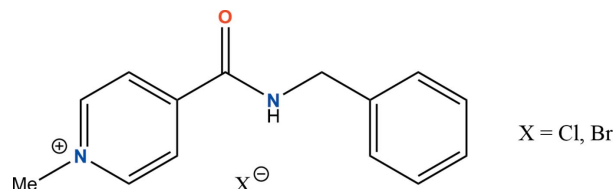
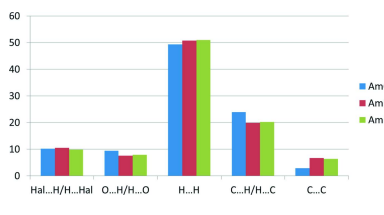
<sup>a</sup>SSI "Institute for Single Crystals", NAS of Ukraine, 60 Nauky ave., Kharkiv, 61001, Ukraine, <sup>b</sup>V.N. Karazin Kharkiv National University, 4 Svobody sq., Kharkiv, 61022, Ukraine, <sup>c</sup>Farmak JSC, 63 Kyrylivska str., Kyiv, 04080, Ukraine, and <sup>d</sup>Kyiv National Technical University of Ukraine, 37 Pobedy ave., Kyiv, 03056, Ukraine. \*Correspondence e-mail: sveta@xray.isc.kharkov.com

Two salts of 4-[(benzylamino)carbonyl]-1-methylpyridinium (**Am**) with chloride ( $C_{14}H_{15}N_2O^+\cdot Cl^-$ ) and bromide ( $C_{14}H_{15}N_2O^+\cdot Br^-$ ) anions were studied and compared with the iodide salt. **AmCl** crystallizes in the centrosymmetric space group  $P2_1/n$  while **AmBr** and **AmI** form crystals in the Sohncke space group  $P2_12_12_1$ . Crystals of **AmBr** are isostructural to those of **AmI**. The cation and anion are bound by an N–H...Hal hydrogen bond. Hirshfeld surface analysis was used to compare different types of intermolecular interactions in the three structures under study.

### 1. Chemical context

Organic salts are of great importance for the pharmaceutical industry (Stahl & Wermuth, 2002). Many drugs are produced in the form of salts because of their higher solubility as compared to neutral compounds. The pharmacokinetic properties may be modified by the choice of counter-ion (Guerrieri *et al.*, 2010; He *et al.*, 2018). Therefore, the study of the ability of an active pharmaceutical ingredient to form salts with different ions is an actual problem.

4-[(Benzylamino)carbonyl]-1-methylpyridinium iodide is known as a multimodal antiviral drug (Buhtiarova *et al.*, 2003; Frolov *et al.*, 2004; Boltz *et al.*, 2018; Cocking *et al.*, 2018). This salt crystallized in the  $P2_12_12_1$  orthorhombic space group and was studied by single-crystal X-ray diffraction, powder diffraction, IR spectroscopy and DSC (Drebushchak *et al.*, 2017). Screening varying different solvents and crystallization conditions did not reveal the formation of any other polymorphs.



In the present work we studied salts of the 4-[(benzylamino)carbonyl]-1-methylpyridinium cation with chloride and bromide anions and compared their molecular and crystal structures with that of the iodide salt.



OPEN ACCESS

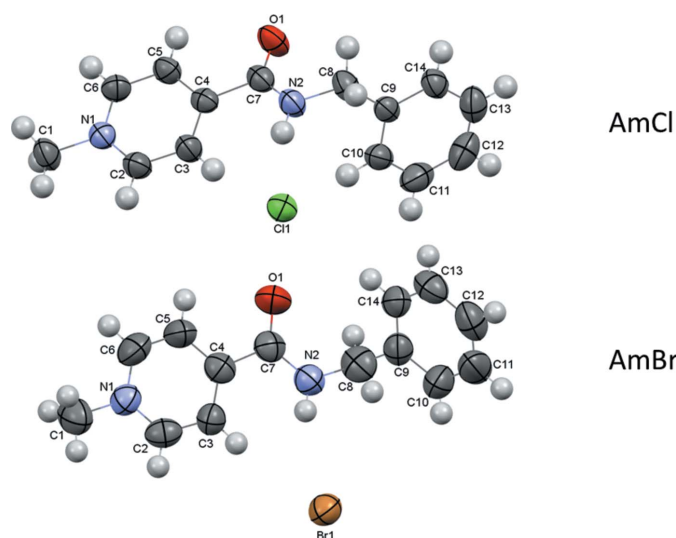


**Figure 1**  
Molecular structures of the title 4-[(benzylamino)carbonyl]-1-methylpyridinium halogenide salts. Displacement ellipsoids are shown with 50% probability level.

## 2. Structural commentary

Usually organic salts are obtained following hydrogen transfer within an acid–base pair. The equilibrium between the neutral acid–base pair and their cation–anion pair depends on external conditions such as temperature, concentration, nature of solvent, etc (Stahl & Nakano, 2002). As a result, organic cations formed upon protonation are not stable and can be deprotonated. The quaternization of the pyridine nitrogen atom also results in cation formation (Wei *et al.*, 2018). However, such a cation is much more stable than its protonated analogue and can form salts with different anions.

The organic cation is formed due to the quaternization of the pyridine moiety in the two salts under study (Fig. 1). The positive charge is located at the pyridine nitrogen atom. The carbamide group and the pyridine ring are slightly non-coplanar in the chloride salt and coplanar in the bromide salt

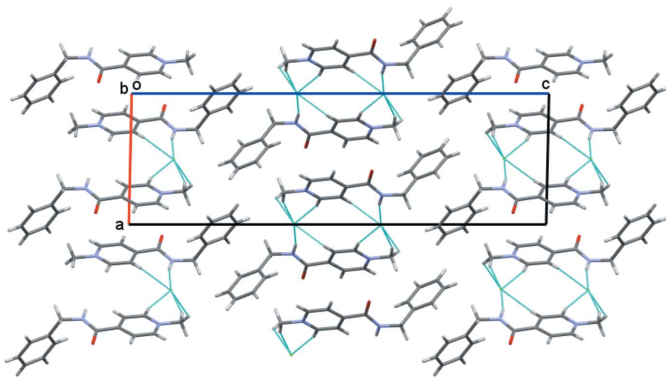


**Figure 2**  
Crystal structure of 4-[(benzylamino)carbonyl]-1-methylpyridinium chloride.  $X\text{--H}\cdots\text{Cl}$  hydrogen bonds are shown as dashed cyan lines.

[the  $\text{C}5\text{--C}4\text{--C}7\text{--O}1$  torsion angle is  $-13.3(4)^\circ$  in **AmCl** and  $-1.4(16)^\circ$  in **AmBr**]. The intramolecular contacts  $\text{H}2\cdots\text{C}3 = 2.57 \text{ \AA}$ ,  $\text{H}2\cdots\text{H}3 = 2.05 \text{ \AA}$  in **AmCl** and  $\text{H}2\cdots\text{C}3 = 2.65 \text{ \AA}$ ,  $\text{H}2\cdots\text{H}3 = 2.16 \text{ \AA}$  in **AmBr** are shorter than the sums of the corresponding van der Waals radii ( $\text{H}\cdots\text{C} = 2.87 \text{ \AA}$  and  $\text{H}\cdots\text{H} = 2.34 \text{ \AA}$ ; Zefirov, 1997) and point to a steric repulsion between the carbamide and pyridine fragments in the cations of **AmCl** and **AmBr**. The phenyl fragment of the benzyl substituent is positioned orthogonally to the carbamide unit and rotated around the  $\text{N}2\text{--C}8$  bond [the  $\text{C}7\text{--N}2\text{--C}8\text{--C}9$  torsion angle is  $-88.1(4)^\circ$  in **AmCl** and  $93.5(12)^\circ$  in **AmBr** while the  $\text{N}2\text{--C}8\text{--C}9\text{--C}10$  torsion angle is  $-24.3(4)^\circ$  in **AmCl** and  $103.8(12)^\circ$  in **AmBr**].

The **AmCl** salt crystallizes in the centrosymmetric  $P2_1/n$  space group while the **AmBr** salt crystallizes in the Sohncke space group  $P2_12_12_1$ , similar to the **AmI** salt (Drebushchak *et al.*, 2017). The cation does not contain an asymmetric atom.

## 3. Supramolecular features

Analysis of the intermolecular interactions revealed that an  $\text{N--H}\cdots\text{Hal}$  intermolecular hydrogen bond is present in both of the salts under study (Tables 1 and 2). This hydrogen bond

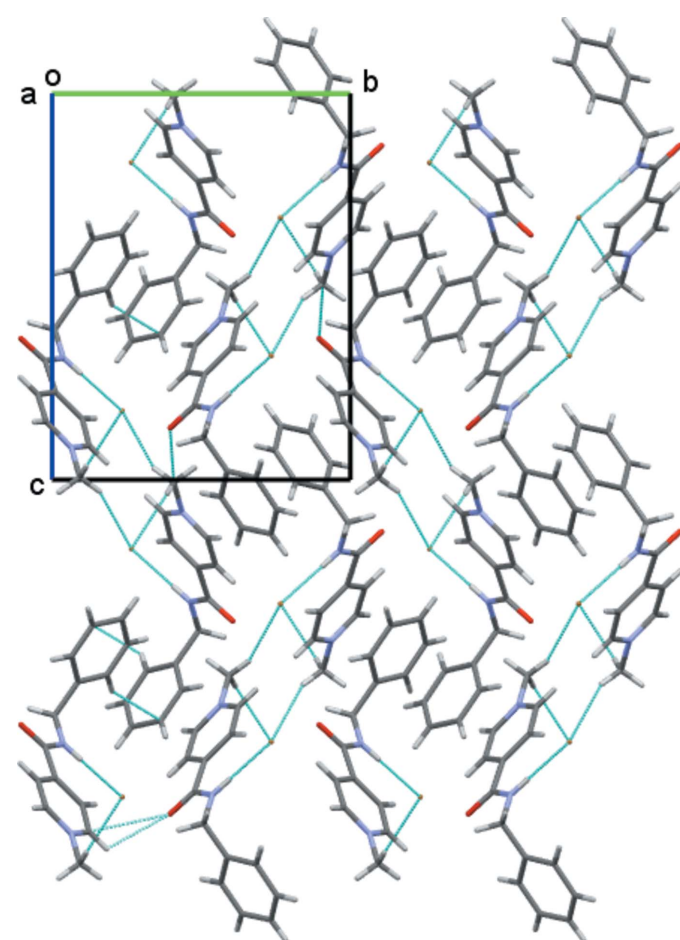


**Figure 3**  
Crystal structure of 4-[(benzylamino)carbonyl]-1-methylpyridinium bromide.  $X\text{--H}\cdots\text{Br}$  hydrogen bonds are shown as dashed cyan lines.

**Table 1**  
Hydrogen-bond geometry ( $\text{\AA}$ ,  $^\circ$ ) for **AmCl**.

$D-\text{H}\cdots A$	$D-\text{H}$	$\text{H}\cdots A$	$D\cdots A$	$D-\text{H}\cdots A$
N2—H2 $\cdots$ Cl1	0.92 (3)	2.26 (3)	3.163 (3)	165 (2)
C1—H1C $\cdots$ Cl1 <sup>i</sup>	0.96	2.89	3.513 (3)	124
C1—H1A $\cdots$ Cl1 <sup>ii</sup>	0.96	2.72	3.633 (3)	160
C2—H2A $\cdots$ Cl1 <sup>ii</sup>	0.93	2.59	3.474 (3)	160
C3—H3 $\cdots$ Cl1	0.93	2.63	3.531 (3)	165

Symmetry codes: (i)  $-x + 2, -y + 1, -z + 1$ ; (ii)  $-x + 2, -y + 2, -z + 1$ .

**Table 2**  
Hydrogen-bond geometry ( $\text{\AA}$ ,  $^\circ$ ) for **AmBr**.

$D-\text{H}\cdots A$	$D-\text{H}$	$\text{H}\cdots A$	$D\cdots A$	$D-\text{H}\cdots A$
N2—H2 $\cdots$ Br1	0.86	2.68	3.468 (9)	154
C1—H1A $\cdots$ Br1 <sup>i</sup>	0.96	3.04	3.913 (13)	152
C1—H1C $\cdots$ Br1 <sup>ii</sup>	0.96	3.01	3.901 (13)	154

Symmetry codes: (i)  $x - \frac{1}{2}, -y + \frac{1}{2}, -z$ ; (ii)  $x - 1, y, z$ .

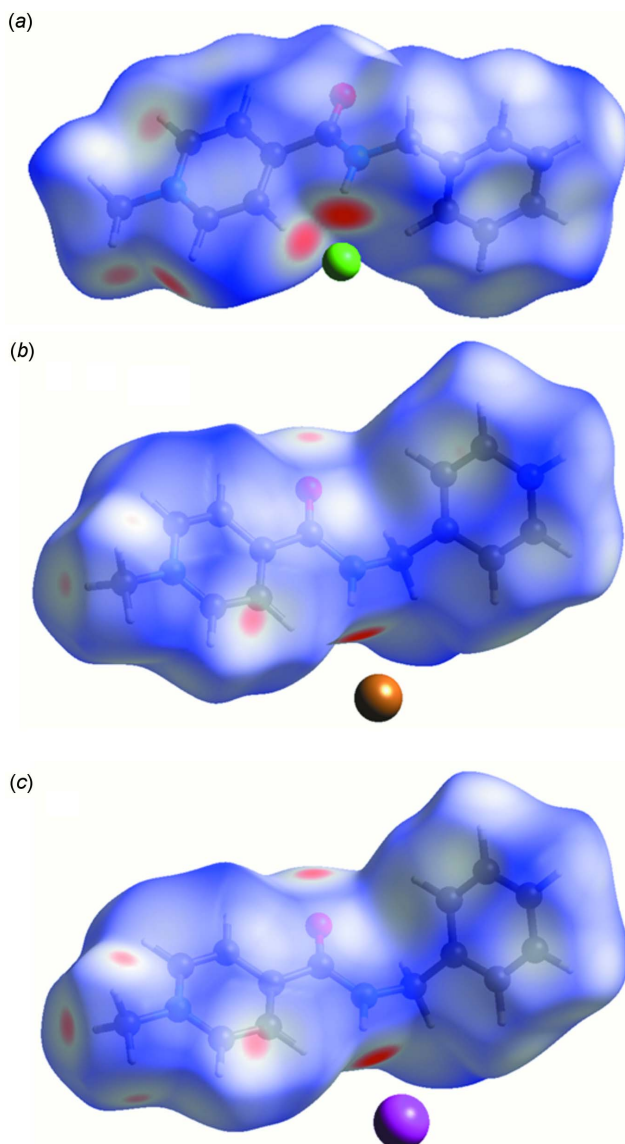


**Figure 4**  
Hirshfeld surfaces of the cation in the (a) **AmCl**, (b) **AmBr** and (c) **AmI** salts mapped over  $d_{\text{norm}}$ .

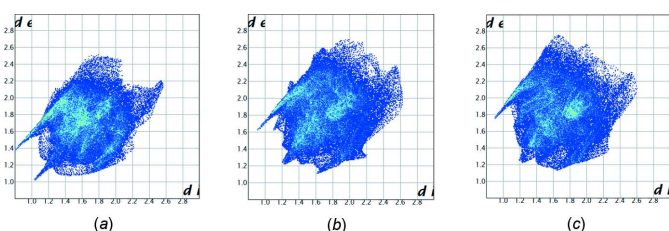


**Figure 5**

Two-dimensional fingerprint plots for the cation in the three salts under study: (a) **AmCl**, (b) **AmBr** and (c) **AmI**.

is strongest in the **AmCl** salt as a result of the higher negativity of chloride anions as compared to bromide and iodide counter-ions. In addition, a set of C—H $\cdots$ Cl' intermolecular hydrogen bonds is found in **AmCl** (Fig. 2) while only two C—H $\cdots$ Hal' hydrogen bonds are present in the crystal structure of **AmBr** (Figs. 3 and 4; Tables 1 and 2). Generally, the presence of pyridine and benzene rings in a molecule can lead to the formation of  $\pi$ — $\pi$  stacking interactions in the crystalline phase. However, no such stacking interactions were found in the **AmCl** and **AmBr** crystals.

#### 4. Hirshfeld surface analysis

The formation of intermolecular interactions in the two salts under study and the **AmI** salt can be compared using Hirshfeld surface analysis and two-dimensional fingerprint plots [Turner *et al.*, 2017]. The Hirshfeld surfaces were obtained for the cations using a standard high surface resolution, mapped over  $d_{\text{norm}}$ . The red spots on the  $d_{\text{norm}}$  surfaces correspond to contacts that are shorter than the van der Waals radii sum of the closest atoms (Fig. 4). Such red spots are observed on all the hydrogen atoms participating in the above-mentioned intermolecular hydrogen bonds (Tables 1 and 2). It should be noted that the brightness of the spot on the hydrogen atom decreases with an increase in the radius of the halogen atom, indicating a weakening of the hydrogen bond.

The hydrogen bonds and short contacts of the cations found in the structures of **AmCl**, **AmBr** and **AmI** are shown in the two-dimensional fingerprint plots presented in Fig. 5a–c. It should be noted that the fingerprint plots constructed for the

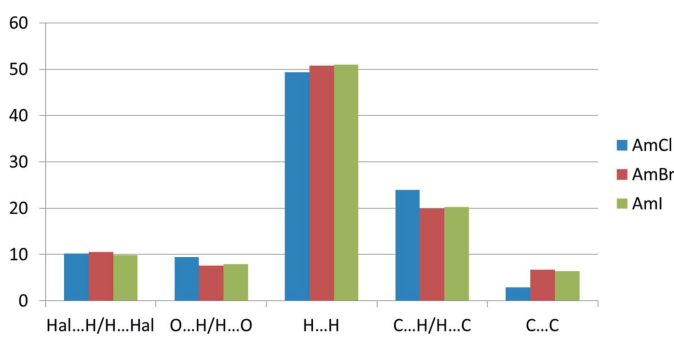


**Figure 6**

Contributions of the different types of interactions to the total Hirshfeld surface of the cation in three halogenide salts.

**Table 3**

Characteristic vibration frequencies according to the FTIR data.

Location of bond	Vibrations	<b>AmCl</b> , wavenumbers	<b>AmBr</b> , wavenumbers
Valence vibrations of monosubstituted amides	N—H (stretching)	3166	3198
Valence vibrations (aromatic system)	C—H (stretching)	3049	3042
Valence vibrations ( $\text{CH}_3$ )	C—H (stretching)	2994	3001
Valence vibrations of the carboxyl group in amides	C=O (stretching)	1656, 1572	1659, 1571
Vibrations of bonds in the pyridine ring	C—H (out-of-plane bending)	727, 659	702, 621

cations in structures **AmBr** and **AmI** are very similar (Fig. 5*b* and 5*c*). The main contribution to the total Hirshfeld surface (49.4% in **AmCl**, 50.8% in **AmBr**, 51.0% in **AmI**) is provided by H···H short contacts (Fig. 6). The contribution of C···H/H···C contacts is much smaller but also significant (23.9% in **AmCl**, 19.9% in **AmBr**, 20.2% in **AmI**). The similar contributions of Hal···H/H···Hal contacts (10.2% in **AmCl**, 10.5% in **AmBr**, 9.9% in **AmI**) and O···H/H···O contacts (9.4% in **AmCl**, 7.6% in **AmBr**, 7.9% in **AmI**) are slightly surprising because of the absence of X—H···O intermolecular interactions in the structures under study. The presence of two aromatic rings in the cation could result in the formation of stacking interactions in the crystal, but the contribution of the C···C contacts is the smallest (2.9% in **AmCl**, 6.7% in **AmBr**, 6.4% in **AmI**). The small contribution of the C···C contacts agrees with the results of the traditional analysis of intermolecular interactions in a crystal using the shortest distances between atoms belonging to neighbouring molecules (see *Supramolecular features* section). It should be noted that the contribution of the C···C contacts is more than twice as high in the crystals of **AmBr** and **AmI** compared to **AmCl**. This can be explained by a mutual orientation of the pyridine and benzene rings belonging to neighbouring molecules in the **AmBr** and **AmI** crystals. However, there are no effective  $\pi$ – $\pi$  interaction between these rings because the distances and angles between the planar  $\pi$  systems are too large.

## 5. Database survey

A search of the Cambridge Structural Database (Version 5.42, update of November 2020; Groom *et al.*, 2016) revealed the structure of the **AmI** salt (refcode BEBFIA; Drebushchak *et al.*, 2017). A comparison with the **AmBr** and **AmI** crystal structures showed that they are isostructural.

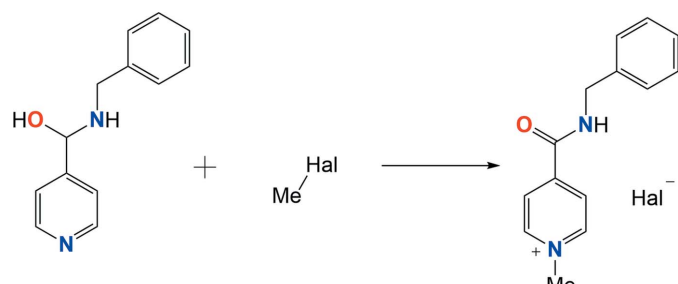
## 6. Synthesis and crystallization

The synthesis of salts of 4-[(benzylamino)carbonyl]-1-methylpyridinium halide was carried out according to the reaction scheme below.

### Synthesis and crystallization of **AmCl**.

520 mL of acetonitrile was cooled to 273–277 K in a glass flask. Chloromethane (87.8 g, 1.739 mol) was dissolved at this temperature. Benzylamide isonicotinic acid (245.78 g, 1.16 mol) and 600 mL of cooled acetonitrile and acetonitrile solution saturated with chloromethane were loaded into an autoclave. The autoclave was closed and heated to 373 K. The

mixture was incubated for 3 h at this temperature. After that, the mixture was allowed to cool to room temperature. The reaction mixture was transferred into a glass flask and cooled to 273–275 K. The reaction mixture was filtered and the precipitate was rinsed on the filter with 200 mL of cooled acetonitrile. The product was dried at 313 K for 12 h. Yield 226 g of crude 4-[(benzylamino)carbonyl]-1-methylpyridinium chloride (75%); white crystals.



226 g of crude 4-[(benzylamino)carbonyl]-1-methylpyridinium chloride were dissolved in 265 mL of 90% ethanol and 660 mL of 2-propanol, and 4.25 g activated charcoal were added. The reaction mixture was heated to boiling point, stirred at boiling for 30 min and filtered. The obtained solution was let to spontaneously cool to a temperature of 303 K, then to a temperature of 278–283 K in a cooling water bath, and stirred for 2 h at this temperature. The reaction mixture was filtrated and the precipitate rinsed on the filter with 110 mL of cold 2-propanol. The product was dried at 313 K for 12 h. Yield 180.8 g of 4-[(benzylamino)carbonyl]-1-methylpyridinium chloride (80%); white crystals; m.p. 474–477 K.

### Synthesis and crystallization of **AmBr**.

4-[(Benzylamino)carbonyl]-1-methylpyridinium iodide (57.7 g, 0.163 mol), silver bromide (33.77 g, 0.180 mol) and 700 mL of water were loaded into a glass flask. The mixture was stirred for 72 h. The sediment was filtered off. The solvent was evaporated under reduced pressure. 300 mL of acetonitrile were added to the precipitate and the mixture was refluxed for 2 h. The reaction mixture was allowed to spontaneously cool to a temperature of 303 K. The reaction mixture was filtered and the precipitate was rinsed on the filter with 50 mL of cold acetonitrile. The product was dried at 313 K for 12 h. Yield 14 g of 4-[(benzylamino)carbonyl]-1-methylpyridinium bromide (28%); white crystals; m.p. 465–468 K.

The crystals of **AmCl** and **AmBr** were grown as very small colourless and yellow parallelepipeds, respectively, in contrast to the well-grown yellow block-shaped crystals of **AmI**.

**Table 4**  
Experimental details.

	<b>AmCl</b>	<b>AmBr</b>
Crystal data		
Chemical formula	$C_{14}H_{15}N_2O^+\cdot Cl^-$	$C_{14}H_{15}N_2O^+\cdot Br^-$
$M_r$	262.73	307.19
Crystal system, space group	Monoclinic, $P2_1/n$	Orthorhombic, $P2_12_12_1$
Temperature (K)	293	293
$a, b, c$ (Å)	8.5222 (7), 5.6875 (3), 27.1720 (14)	9.417 (3), 11.099 (5), 14.363 (6)
$\alpha, \beta, \gamma$ (°)	90, 91.243 (6), 90	90, 90, 90
$V$ (Å $^3$ )	1316.71 (15)	1501.2 (10)
$Z$	4	4
Radiation type	Mo $K\alpha$	Mo $K\alpha$
$\mu$ (mm $^{-1}$ )	0.28	2.73
Crystal size (mm)	0.30 × 0.20 × 0.10	0.30 × 0.30 × 0.06
Data collection		
Diffractometer	Xcalibur, Sapphire3	Xcalibur, Sapphire3
Absorption correction	Multi-scan ( <i>CrysAlis PRO</i> , Rigaku OD 2018)	Multi-scan ( <i>CrysAlis PRO</i> , Rigaku OD 2018)
$T_{min}, T_{max}$	0.624, 1.000	0.068, 1.000
No. of measured, independent and observed [ $I > 2\sigma(I)$ ] reflections	5343, 2302, 1529	10683, 2635, 1583
$R_{int}$	0.048	0.118
(sin $\theta/\lambda$ ) $_{max}$ (Å $^{-1}$ )	0.595	0.594
Refinement		
$R[F^2 > 2\sigma(F^2)], wR(F^2), S$	0.051, 0.119, 1.05	0.063, 0.150, 1.00
No. of reflections	2302	2635
No. of parameters	168	164
H-atom treatment	H atoms treated by a mixture of independent and constrained refinement	H-atom parameters constrained
$\Delta\rho_{max}, \Delta\rho_{min}$ (e Å $^{-3}$ )	0.18, -0.16	0.34, -0.60
Absolute structure	-	Flack $x$ determined using 407 quotients [( $I^+ - I^-$ )]/[ $(I^+ + I^-)$ ] (Parsons <i>et al.</i> , 2013) 0.00 (2)
Absolute structure parameter	-	

Computer programs: *CrysAlis PRO* (Rigaku OD, 2018), *SHELXT2014/5* (Sheldrick, 2015a), *SHELXL2016/6* (Sheldrick, 2015b), *Mercury* (Macrae *et al.*, 2020) and *OLEX2* (Dolomanov *et al.*, 2009).

## 7. Spectroscopic characterization

Both salts under consideration were fully characterized by IR,  $^1H$  NMR and  $^{13}C$  NMR spectroscopy. IR spectra of solid samples were acquired on a Thermo Fisher Scientific Nicolet iS50 FTIR spectrometer.  $^1H$  NMR spectra of samples were measured in DMSO- $d_6$  on a 600 MHz Varian spectrometer.  $^{13}C$  NMR spectra of samples were taken in DMSO- $d_6$  on a 150 MHz Varian spectrometer.

The characteristic vibration frequencies of the main functional groups according to the data of FTIR spectroscopy are shown in Table 3. The full spectroscopic data are presented below and in Figs. 7 and 8. As can be seen from Table 3, the

main difference in IR spectra concerns the valence vibrations of the N–H group and vibrations of C–H bonds in the pyridine ring.

### AmCl:

IR spectrum (cm $^{-1}$ ) (Fig. 7): 592.40, 631.16, 659.97, 667.17, 702.46, 727.71, 857.87, 890.80, 989.03, 1156.13, 1229.22, 1260.13, 1284.00, 1305.82, 1312.72, 1342.62, 1416.08, 1453.14, 1497.17, 1516.77, 1572.84, 1656.90, 2981.77, 2994.48, 3009.82, 3049.81, 3166.99.

$^1H$  NMR (600 MHz, DMSO- $d_6$ , p.p.m.):  $\delta$  = 4.40 (s, 3H, CH $_3$ ), 4.48–4.49 (d, 2H, CH $_2$ ), 7.21–7.36 (m, 5H, Ar), 8.59 (d, 2H, Py), 9.21 (d, 2H, Py), 10.47 (s, H, NH).

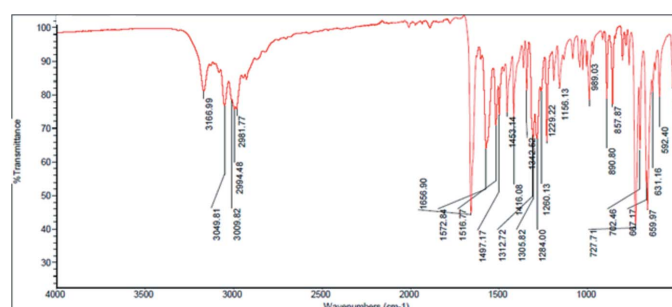


**Figure 7**  
IR spectrum of the **AmCl** salt.

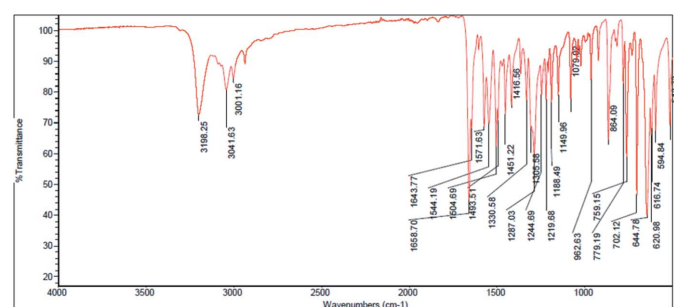


**Figure 8**  
IR spectrum of the **AmBr** salt.

<sup>13</sup>C NMR (150 MHz, DMSO-*d*<sub>6</sub>, p.p.m.): δ = 43.42 (CH<sub>2</sub>), 48.37 (CH<sub>3</sub>), 125.98, 146.94, 147.91 (Py), 127.44, 128.00, 128.75, 139.03 (Ar), 162.12 (C=O).

#### AmBr:

IR spectrum (cm<sup>-1</sup>) (Fig. 8): 594.84, 616.74, 620.98, 644.78, 702.12, 759.15, 779.19, 864.09, 962.63, 1079.02, 1149.96, 1188.49, 1219.68, 1244.69, 1287.03, 1305.58, 1330.58, 1416.56, 1451.22, 1493.51, 1504.69, 1544.19, 1571.63, 1643.77, 1658.70, 3001.16, 3041.63, 3198.25.

<sup>1</sup>H NMR (400 MHz, DMSO-*d*<sub>6</sub>, p.p.m.): δ = 4.41 (*s*, 3H, CH<sub>3</sub>), 4.51 (*d*, 2H, CH<sub>2</sub>), 7.23–7.36 (*m*, 5H, Ar), 8.48 (*d*, 2H, Py), 9.21 (*d*, 2H, Py), 9.92 (*s*, H, NH).

<sup>13</sup>C NMR (100 MHz, DMSO-*d*<sub>6</sub>, p.p.m.): δ = 43.52 (CH<sub>2</sub>), 48.50 (CH<sub>3</sub>), 125.87, 146.99, 147.97 (Py), 127.56, 128.00, 128.84, 138.83 (Ar), 162.31 (C=O).

## 8. Refinement

Crystal data, data collection and structure refinement details are summarized in Table 4. All of the hydrogen atoms were located in difference-Fourier maps. They were included in calculated positions and treated as riding with C—H = 0.96 Å, *U*<sub>iso</sub>(H) = 1.5*U*<sub>eq</sub> for methyl groups and with C<sub>ar</sub>—H = 0.93 Å, *Csp*<sup>2</sup>—H = 0.97 Å, *U*<sub>iso</sub>(H) = 1.2*U*<sub>eq</sub> for all other hydrogen atoms.

## Acknowledgements

The authors are grateful to Farmak JSC for support of this work.

## Funding information

Funding for this research was provided by: National Academy of Sciences of Ukraine (grant No. 0120U102660).

## References

- Boltz, D., Peng, X., Muzzio, M., Dash, P., Thomas, P. G. & Margitich, V. (2018). *Antivir. Chem. Chemother.* pp. 26 <https://doi.org/10.1177/2040206618811416>
- Buhtiarova, T. A., Danilenko, V. P., Homenko, V. S., Shatyrkina, T. V. & Yadlovsky, O. E. (2003). *Ukrainian Med. J.* **33**, 72–74.
- Cocking, D., Cinatl, J., Boltz, D. A., Peng, X., Johnson, W., Muzzio, M., Syarkevych, O., Kostyuk, G., Goy, A., Mueller, L. & Margitich, V. (2018). *Acta Virol.* **62**, 191–195.
- Dolomanov, O. V., Bourhis, L. J., Gildea, R. J., Howard, J. A. K. & Puschmann, H. (2009). *J. Appl. Cryst.* **42**, 339–341.
- Drebushchak, T. N., Kryukov, Y. A., Rogova, A. I. & Boldyreva, E. V. (2017). *Acta Cryst. E73*, 967–970.
- Frolov, A. F., Frolov, V. M., Buhtiarova, T. A. & Danilenko, V. P. (2004). *Ukrainian Med. J.* **39**, 69–74.
- Groom, C. R., Bruno, I. J., Lightfoot, M. P. & Ward, S. C. (2016). *Acta Cryst. B72*, 171–179.
- Guerrieri, P., Jarring, K. & Taylor, L. S. (2010). *J. Pharm. Sci.* **99**, 3719–3730.
- He, Y., Orton, E. & Yang, D. (2018). *J. Pharm. Sci.* **107**, 419–425.
- Macrae, C. F., Sovago, I., Cottrell, S. J., Galek, P. T. A., McCabe, P., Pidcock, E., Platings, M., Shields, G. P., Stevens, J. S., Towler, M. & Wood, P. A. (2020). *J. Appl. Cryst.* **53**, 226–235.
- Parsons, S., Flack, H. D. & Wagner, T. (2013). *Acta Cryst. B69*, 249–259.
- Rigaku OD (2018). *CrysAlis PRO*. Rigaku Oxford Diffraction, Yarnton, England.
- Sheldrick, G. M. (2015a). *Acta Cryst. A71*, 3–8.
- Sheldrick, G. M. (2015b). *Acta Cryst. A71*, 3–8.
- Stahl, P. H. & Nakano, M. (2002). In *Handbook of Pharmaceutical Salts: Properties, Selection, and Use* edited by P. H. Stahl & C. G. Wermuth, pp. 83–116. Weinheim: Wiley-VCH.
- Stahl, P. H. & Wermuth, C. G. (2002). *Handbook of Pharmaceutical Salts: Properties, Selection, and Use*. Weinheim: Wiley-VCH.
- Turner, M. J., McKinnon, J. J., Wolff, S. K., Grimwood, D. J., Spackman, P. R., Jayatilaka, D. & Spackman, M. A. (2017). *CrystalExplorer17*. University of Western Australia. <http://Hirshfeldsurface.net>
- Wei, L., Chen, Y., Tan, W., Li, Q., Gu, G., Dong, F. & Guo, Z. (2018). *Molecules*, **23**, 2604–2616.
- Zefirov, Yu. V. (1997). *Kristallografiya*, **42**, 936–958.

# supporting information

*Acta Cryst.* (2022). E78, 114-119 [https://doi.org/10.1107/S2056989021013505]

## 4-[(Benzylamino)carbonyl]-1-methylpyridinium halogenide salts: X-ray diffraction study and Hirshfeld surface analysis

Svitlana V. Shishkina, Anna M. Shaposhnik, Vyacheslav M. Baumer, Vitalii V. Rudiuk and Igor A. Levandovskiy

### Computing details

For both structures, data collection: *CrysAlis PRO* (Rigaku OD, 2018); cell refinement: *CrysAlis PRO* (Rigaku OD, 2018); data reduction: *CrysAlis PRO* (Rigaku OD, 2018); program(s) used to solve structure: *SHELXT2014/5* (Sheldrick, 2015a); program(s) used to refine structure: *SHELXL2016/6* (Sheldrick, 2015b); molecular graphics: *Mercury* (Macrae *et al.*, 2020); software used to prepare material for publication: *OLEX2* (Dolomanov *et al.*, 2009).

### 4-[(Benzylamino)carbonyl]-1-methylpyridinium chloride (AmCl)

#### Crystal data

$\text{C}_{14}\text{H}_{15}\text{N}_2\text{O}^+\cdot\text{Cl}^-$   
 $M_r = 262.73$   
Monoclinic,  $P2_1/n$   
 $a = 8.5222$  (7) Å  
 $b = 5.6875$  (3) Å  
 $c = 27.1720$  (14) Å  
 $\beta = 91.243$  (6)°  
 $V = 1316.71$  (15) Å<sup>3</sup>  
 $Z = 4$

$F(000) = 552$   
 $D_x = 1.325 \text{ Mg m}^{-3}$   
Mo  $K\alpha$  radiation,  $\lambda = 0.71073$  Å  
Cell parameters from 766 reflections  
 $\theta = 3.2\text{--}20.4^\circ$   
 $\mu = 0.28 \text{ mm}^{-1}$   
 $T = 293$  K  
Block, colorless  
 $0.30 \times 0.20 \times 0.10$  mm

#### Data collection

Xcalibur, Sapphire3  
diffractometer  
Radiation source: Enhance (Mo) X-ray Source  
Detector resolution: 16.1827 pixels mm<sup>-1</sup>  
 $\omega$  scans  
Absorption correction: multi-scan  
(CrysAlisPro, Rigaku OD 2018)  
 $T_{\min} = 0.624$ ,  $T_{\max} = 1.000$

5343 measured reflections  
2302 independent reflections  
1529 reflections with  $I > 2\sigma(I)$   
 $R_{\text{int}} = 0.048$   
 $\theta_{\max} = 25.0^\circ$ ,  $\theta_{\min} = 3.0^\circ$   
 $h = -10 \rightarrow 9$   
 $k = -6 \rightarrow 6$   
 $l = -31 \rightarrow 26$

#### Refinement

Refinement on  $F^2$   
Least-squares matrix: full  
 $R[F^2 > 2\sigma(F^2)] = 0.051$   
 $wR(F^2) = 0.119$   
 $S = 1.05$   
2302 reflections  
168 parameters  
0 restraints

Hydrogen site location: mixed  
H atoms treated by a mixture of independent  
and constrained refinement  
 $w = 1/[\sigma^2(F_o^2) + (0.034P)^2]$   
where  $P = (F_o^2 + 2F_c^2)/3$   
 $(\Delta/\sigma)_{\max} < 0.001$   
 $\Delta\rho_{\max} = 0.18 \text{ e } \text{\AA}^{-3}$   
 $\Delta\rho_{\min} = -0.16 \text{ e } \text{\AA}^{-3}$

*Special details*

**Geometry.** All esds (except the esd in the dihedral angle between two l.s. planes) are estimated using the full covariance matrix. The cell esds are taken into account individually in the estimation of esds in distances, angles and torsion angles; correlations between esds in cell parameters are only used when they are defined by crystal symmetry. An approximate (isotropic) treatment of cell esds is used for estimating esds involving l.s. planes.

*Fractional atomic coordinates and isotropic or equivalent isotropic displacement parameters ( $\text{\AA}^2$ )*

	<i>x</i>	<i>y</i>	<i>z</i>	$U_{\text{iso}}^*/U_{\text{eq}}$
C11	1.00363 (10)	0.87872 (14)	0.60412 (3)	0.0644 (3)
O1	0.5912 (3)	0.1775 (4)	0.57992 (7)	0.0685 (7)
N1	0.7393 (3)	0.5404 (4)	0.42221 (8)	0.0507 (6)
N2	0.7762 (3)	0.4394 (5)	0.60568 (9)	0.0568 (7)
H2	0.844 (4)	0.561 (5)	0.5990 (10)	0.063 (10)*
C1	0.7545 (4)	0.6081 (6)	0.37003 (9)	0.0661 (10)
H1A	0.822085	0.742522	0.367808	0.099*
H1B	0.652886	0.646109	0.356333	0.099*
H1C	0.798499	0.479503	0.352058	0.099*
C2	0.8023 (4)	0.6758 (5)	0.45742 (10)	0.0586 (9)
H2A	0.855209	0.812634	0.449031	0.070*
C3	0.7896 (4)	0.6142 (5)	0.50613 (10)	0.0594 (9)
H3	0.833718	0.709994	0.530460	0.071*
C4	0.7124 (3)	0.4127 (5)	0.51914 (10)	0.0469 (7)
C5	0.6493 (4)	0.2765 (5)	0.48176 (10)	0.0551 (8)
H5	0.595346	0.139381	0.489249	0.066*
C6	0.6655 (4)	0.3418 (5)	0.43357 (11)	0.0575 (9)
H6	0.624699	0.246639	0.408589	0.069*
C7	0.6881 (4)	0.3322 (5)	0.57169 (11)	0.0535 (8)
C8	0.7728 (4)	0.3762 (5)	0.65733 (9)	0.0603 (9)
H8A	0.875072	0.408118	0.672190	0.072*
H8B	0.754012	0.208480	0.659881	0.072*
C9	0.6503 (4)	0.5038 (5)	0.68622 (9)	0.0492 (8)
C10	0.5909 (4)	0.7194 (5)	0.67180 (11)	0.0589 (9)
H10	0.626455	0.789378	0.643179	0.071*
C11	0.4807 (5)	0.8315 (6)	0.69903 (12)	0.0763 (11)
H11	0.441586	0.976239	0.688610	0.092*
C12	0.4267 (5)	0.7325 (7)	0.74176 (13)	0.0789 (11)
H12	0.349989	0.808053	0.759759	0.095*
C13	0.4875 (4)	0.5203 (7)	0.75753 (11)	0.0732 (11)
H13	0.454056	0.453721	0.786750	0.088*
C14	0.5986 (4)	0.4067 (6)	0.72969 (10)	0.0587 (9)
H14	0.638986	0.263078	0.740336	0.070*

*Atomic displacement parameters ( $\text{\AA}^2$ )*

	$U^{11}$	$U^{22}$	$U^{33}$	$U^{12}$	$U^{13}$	$U^{23}$
C11	0.0722 (6)	0.0577 (5)	0.0636 (5)	-0.0109 (5)	0.0095 (4)	-0.0002 (4)
O1	0.0690 (16)	0.0706 (15)	0.0660 (14)	-0.0208 (14)	0.0031 (12)	0.0193 (11)

N1	0.0510 (16)	0.0512 (15)	0.0500 (14)	0.0014 (14)	0.0027 (12)	0.0026 (12)
N2	0.0646 (19)	0.0573 (17)	0.0487 (15)	-0.0113 (16)	0.0033 (14)	0.0087 (13)
C1	0.078 (3)	0.075 (2)	0.0447 (16)	-0.012 (2)	-0.0035 (16)	0.0126 (15)
C2	0.070 (2)	0.0507 (19)	0.0552 (19)	-0.0110 (18)	-0.0021 (17)	0.0057 (15)
C3	0.075 (2)	0.0558 (19)	0.0472 (17)	-0.0142 (19)	-0.0018 (16)	0.0038 (14)
C4	0.0444 (18)	0.0435 (17)	0.0531 (16)	0.0006 (15)	0.0054 (14)	0.0046 (14)
C5	0.055 (2)	0.0516 (18)	0.0588 (18)	-0.0087 (17)	0.0112 (16)	0.0044 (15)
C6	0.062 (2)	0.0515 (19)	0.0585 (19)	-0.0118 (18)	0.0027 (16)	-0.0034 (15)
C7	0.055 (2)	0.0516 (19)	0.0544 (18)	0.0023 (18)	0.0086 (17)	0.0095 (15)
C8	0.064 (2)	0.068 (2)	0.0480 (17)	-0.0007 (19)	-0.0025 (16)	0.0127 (15)
C9	0.056 (2)	0.0489 (18)	0.0422 (15)	-0.0129 (16)	-0.0083 (14)	0.0022 (13)
C10	0.078 (3)	0.0464 (18)	0.0523 (17)	-0.0067 (19)	-0.0081 (17)	0.0038 (15)
C11	0.098 (3)	0.057 (2)	0.073 (2)	0.012 (2)	-0.020 (2)	-0.0109 (18)
C12	0.078 (3)	0.095 (3)	0.064 (2)	0.012 (2)	-0.003 (2)	-0.027 (2)
C13	0.077 (3)	0.094 (3)	0.0485 (18)	-0.012 (2)	0.0034 (19)	-0.0030 (19)
C14	0.069 (2)	0.062 (2)	0.0453 (16)	-0.0060 (19)	-0.0047 (16)	0.0079 (15)

Geometric parameters ( $\text{\AA}$ ,  $^{\circ}$ )

O1—C7	1.230 (3)	C5—H5	0.9300
N1—C6	1.332 (3)	C6—H6	0.9300
N1—C2	1.332 (4)	C8—C9	1.506 (4)
N1—C1	1.478 (3)	C8—H8A	0.9700
N2—C7	1.326 (4)	C8—H8B	0.9700
N2—C8	1.450 (3)	C9—C10	1.380 (4)
N2—H2	0.92 (3)	C9—C14	1.385 (4)
C1—H1A	0.9600	C10—C11	1.366 (4)
C1—H1B	0.9600	C10—H10	0.9300
C1—H1C	0.9600	C11—C12	1.379 (5)
C2—C3	1.376 (4)	C11—H11	0.9300
C2—H2A	0.9300	C12—C13	1.378 (5)
C3—C4	1.372 (4)	C12—H12	0.9300
C3—H3	0.9300	C13—C14	1.385 (4)
C4—C5	1.377 (4)	C13—H13	0.9300
C4—C7	1.518 (4)	C14—H14	0.9300
C5—C6	1.371 (4)		
		O1—C7—N2	125.0 (3)
C6—N1—C2	120.6 (2)	O1—C7—C4	119.5 (3)
C6—N1—C1	119.7 (3)	N2—C7—C4	115.5 (3)
C2—N1—C1	119.7 (3)	N2—C8—C9	114.5 (2)
C7—N2—C8	122.5 (3)	N2—C8—H8A	108.6
C7—N2—H2	123.7 (17)	C9—C8—H8A	108.6
C8—N2—H2	113.8 (17)	N2—C8—H8B	108.6
N1—C1—H1A	109.5	C9—C8—H8B	108.6
N1—C1—H1B	109.5	H8A—C8—H8B	107.6
H1A—C1—H1B	109.5	C10—C9—C14	118.4 (3)
N1—C1—H1C	109.5	C10—C9—C8	122.3 (3)
H1A—C1—H1C	109.5		

H1B—C1—H1C	109.5	C14—C9—C8	119.3 (3)
N1—C2—C3	120.3 (3)	C11—C10—C9	120.9 (3)
N1—C2—H2A	119.9	C11—C10—H10	119.6
C3—C2—H2A	119.9	C9—C10—H10	119.6
C4—C3—C2	120.6 (3)	C10—C11—C12	120.8 (3)
C4—C3—H3	119.7	C10—C11—H11	119.6
C2—C3—H3	119.7	C12—C11—H11	119.6
C3—C4—C5	117.5 (3)	C13—C12—C11	119.3 (3)
C3—C4—C7	124.8 (3)	C13—C12—H12	120.3
C5—C4—C7	117.7 (3)	C11—C12—H12	120.3
C6—C5—C4	120.4 (3)	C12—C13—C14	119.7 (3)
C6—C5—H5	119.8	C12—C13—H13	120.1
C4—C5—H5	119.8	C14—C13—H13	120.1
N1—C6—C5	120.6 (3)	C13—C14—C9	120.9 (3)
N1—C6—H6	119.7	C13—C14—H14	119.5
C5—C6—H6	119.7	C9—C14—H14	119.5
C6—N1—C2—C3	-1.2 (5)	C3—C4—C7—N2	-14.7 (4)
C1—N1—C2—C3	-179.7 (3)	C5—C4—C7—N2	166.9 (3)
N1—C2—C3—C4	0.2 (5)	C7—N2—C8—C9	-88.1 (4)
C2—C3—C4—C5	0.1 (5)	N2—C8—C9—C10	-24.3 (4)
C2—C3—C4—C7	-178.3 (3)	N2—C8—C9—C14	157.9 (3)
C3—C4—C5—C6	0.6 (5)	C14—C9—C10—C11	-1.7 (5)
C7—C4—C5—C6	179.1 (3)	C8—C9—C10—C11	-179.5 (3)
C2—N1—C6—C5	1.9 (5)	C9—C10—C11—C12	0.4 (5)
C1—N1—C6—C5	-179.6 (3)	C10—C11—C12—C13	1.4 (6)
C4—C5—C6—N1	-1.6 (5)	C11—C12—C13—C14	-1.7 (6)
C8—N2—C7—O1	3.0 (5)	C12—C13—C14—C9	0.3 (5)
C8—N2—C7—C4	-177.1 (2)	C10—C9—C14—C13	1.4 (5)
C3—C4—C7—O1	165.2 (3)	C8—C9—C14—C13	179.2 (3)
C5—C4—C7—O1	-13.3 (4)		

*Hydrogen-bond geometry (Å, °)*

D—H···A	D—H	H···A	D···A	D—H···A
N2—H2···Cl1	0.92 (3)	2.26 (3)	3.163 (3)	165 (2)
C1—H1C···Cl1 <sup>i</sup>	0.96	2.89	3.513 (3)	124
C1—H1A···Cl1 <sup>ii</sup>	0.96	2.72	3.633 (3)	160
C2—H2A···Cl1 <sup>ii</sup>	0.93	2.59	3.474 (3)	160
C3—H3···Cl1	0.93	2.63	3.531 (3)	165

Symmetry codes: (i)  $-x+2, -y+1, -z+1$ ; (ii)  $-x+2, -y+2, -z+1$ .**4-[(Benzylamino)carbonyl]-1-methylpyridinium bromide (AmBr)***Crystal data*

$\text{C}_{14}\text{H}_{15}\text{N}_2\text{O}^+\cdot\text{Br}^-$   
 $M_r = 307.19$   
Orthorhombic,  $P2_12_12_1$

$a = 9.417 (3)$  Å  
 $b = 11.099 (5)$  Å  
 $c = 14.363 (6)$  Å

$V = 1501.2 (10) \text{ \AA}^3$   
 $Z = 4$   
 $F(000) = 624$   
 $D_x = 1.359 \text{ Mg m}^{-3}$   
Mo  $K\alpha$  radiation,  $\lambda = 0.71073 \text{ \AA}$   
Cell parameters from 748 reflections

$\theta = 3.2\text{--}24.8^\circ$   
 $\mu = 2.73 \text{ mm}^{-1}$   
 $T = 293 \text{ K}$   
Plate, yellow  
 $0.30 \times 0.30 \times 0.06 \text{ mm}$

#### Data collection

Xcalibur, Sapphire3  
diffractometer  
Radiation source: Enhance (Mo) X-ray Source  
Detector resolution: 16.1827 pixels  $\text{mm}^{-1}$   
 $\omega$  scans  
Absorption correction: multi-scan  
(CrysAlisPro, Rigaku OD 2018)  
 $T_{\min} = 0.068$ ,  $T_{\max} = 1.000$

10683 measured reflections  
2635 independent reflections  
1583 reflections with  $I > 2\sigma(I)$   
 $R_{\text{int}} = 0.118$   
 $\theta_{\max} = 25.0^\circ$ ,  $\theta_{\min} = 3.4^\circ$   
 $h = -11 \rightarrow 11$   
 $k = -13 \rightarrow 13$   
 $l = -17 \rightarrow 16$

#### Refinement

Refinement on  $F^2$   
Least-squares matrix: full  
 $R[F^2 > 2\sigma(F^2)] = 0.063$   
 $wR(F^2) = 0.150$   
 $S = 1.00$   
2635 reflections  
164 parameters  
0 restraints  
Hydrogen site location: inferred from  
neighbouring sites

H-atom parameters constrained  
 $w = 1/[\sigma^2(F_o^2) + (0.0446P)^2]$   
where  $P = (F_o^2 + 2F_c^2)/3$   
 $(\Delta/\sigma)_{\max} < 0.001$   
 $\Delta\rho_{\max} = 0.34 \text{ e \AA}^{-3}$   
 $\Delta\rho_{\min} = -0.60 \text{ e \AA}^{-3}$   
Absolute structure: Flack  $x$  determined using  
407 quotients  $[(I^+)-(I)]/[(I^+)+(I)]$  (Parsons et al.,  
2013)  
Absolute structure parameter: 0.00 (2)

#### Special details

**Geometry.** All esds (except the esd in the dihedral angle between two l.s. planes) are estimated using the full covariance matrix. The cell esds are taken into account individually in the estimation of esds in distances, angles and torsion angles; correlations between esds in cell parameters are only used when they are defined by crystal symmetry. An approximate (isotropic) treatment of cell esds is used for estimating esds involving l.s. planes.

#### Fractional atomic coordinates and isotropic or equivalent isotropic displacement parameters ( $\text{\AA}^2$ )

	$x$	$y$	$z$	$U_{\text{iso}}^*/U_{\text{eq}}$
Br1	0.91899 (12)	0.26554 (10)	0.17853 (8)	0.0849 (5)
O1	0.5589 (10)	0.6049 (7)	0.3657 (5)	0.091 (3)
N2	0.7250 (9)	0.4630 (7)	0.3158 (7)	0.073 (2)
H2	0.743714	0.406610	0.276630	0.088*
N1	0.3008 (10)	0.4355 (9)	0.0832 (7)	0.073 (2)
C7	0.5970 (12)	0.5238 (9)	0.3083 (7)	0.070 (3)
C3	0.5277 (11)	0.3994 (10)	0.1584 (8)	0.071 (3)
H3	0.612742	0.356784	0.159577	0.085*
C2	0.4254 (14)	0.3763 (9)	0.0884 (9)	0.078 (3)
H2A	0.445066	0.317583	0.043984	0.093*
C5	0.3663 (13)	0.5481 (12)	0.2211 (9)	0.090 (4)
H5	0.343497	0.606658	0.264908	0.108*
C4	0.4986 (13)	0.4888 (10)	0.2269 (8)	0.071 (3)
C6	0.2692 (14)	0.5207 (11)	0.1512 (10)	0.095 (4)

H6	0.181979	0.559919	0.149850	0.114*
C9	0.8166 (12)	0.4132 (10)	0.4771 (8)	0.073 (3)
C8	0.8319 (12)	0.4919 (11)	0.3897 (9)	0.090 (4)
H8A	0.821881	0.575832	0.407276	0.108*
H8B	0.926489	0.481169	0.364293	0.108*
C13	0.6899 (13)	0.3640 (12)	0.6235 (8)	0.085 (4)
H13	0.616600	0.379851	0.665032	0.102*
C14	0.7079 (11)	0.4343 (11)	0.5440 (8)	0.073 (3)
H14	0.645855	0.498173	0.534234	0.088*
C12	0.7868 (15)	0.2666 (12)	0.6398 (9)	0.098 (4)
H12	0.776537	0.217390	0.691806	0.118*
C1	0.1934 (12)	0.4075 (14)	0.0071 (9)	0.106 (5)
H1A	0.227194	0.341433	-0.029942	0.158*
H1B	0.180938	0.477098	-0.031718	0.158*
H1C	0.104155	0.386183	0.034937	0.158*
C10	0.9118 (15)	0.3165 (10)	0.4951 (9)	0.096 (4)
H10	0.984059	0.299441	0.453014	0.115*
C11	0.8973 (18)	0.2467 (12)	0.5761 (10)	0.122 (5)
H11	0.962607	0.185674	0.587752	0.147*

*Atomic displacement parameters ( $\text{\AA}^2$ )*

	$U^{11}$	$U^{22}$	$U^{33}$	$U^{12}$	$U^{13}$	$U^{23}$
Br1	0.0782 (7)	0.0895 (8)	0.0868 (8)	0.0122 (7)	0.0041 (7)	0.0018 (7)
O1	0.106 (6)	0.085 (5)	0.083 (6)	0.013 (5)	-0.001 (6)	-0.023 (4)
N2	0.077 (6)	0.074 (6)	0.068 (6)	-0.001 (5)	-0.002 (6)	-0.003 (5)
N1	0.063 (6)	0.077 (7)	0.080 (7)	0.004 (5)	-0.002 (5)	0.000 (5)
C7	0.084 (7)	0.066 (7)	0.060 (7)	0.000 (6)	0.011 (7)	0.014 (5)
C3	0.071 (7)	0.072 (7)	0.071 (8)	0.006 (5)	-0.005 (6)	0.005 (5)
C2	0.077 (7)	0.069 (7)	0.087 (8)	-0.003 (7)	0.020 (8)	-0.004 (5)
C5	0.086 (8)	0.098 (10)	0.086 (9)	0.027 (7)	-0.006 (8)	-0.027 (7)
C4	0.075 (7)	0.071 (8)	0.066 (9)	-0.006 (6)	0.005 (7)	0.004 (6)
C6	0.072 (8)	0.103 (10)	0.111 (12)	0.025 (7)	0.001 (8)	-0.007 (8)
C9	0.078 (8)	0.066 (7)	0.074 (8)	0.000 (6)	-0.012 (7)	0.001 (6)
C8	0.074 (7)	0.102 (10)	0.094 (10)	-0.019 (7)	0.005 (7)	0.000 (7)
C13	0.084 (8)	0.104 (10)	0.065 (8)	-0.015 (8)	0.007 (7)	-0.008 (7)
C14	0.064 (7)	0.082 (8)	0.075 (8)	0.004 (6)	-0.010 (7)	-0.009 (7)
C12	0.126 (10)	0.095 (10)	0.073 (8)	-0.011 (9)	-0.024 (8)	0.007 (8)
C1	0.082 (8)	0.140 (12)	0.095 (10)	-0.004 (9)	-0.009 (8)	-0.014 (9)
C10	0.095 (9)	0.104 (9)	0.088 (9)	0.032 (9)	-0.004 (9)	0.006 (7)
C11	0.178 (15)	0.099 (10)	0.091 (9)	0.059 (12)	-0.027 (11)	-0.014 (8)

*Geometric parameters ( $\text{\AA}$ ,  $^\circ$ )*

O1—C7	1.273 (12)	C9—C14	1.423 (14)
N2—C7	1.386 (12)	C9—C8	1.536 (15)
N2—C8	1.498 (14)	C8—H8A	0.9700
N2—H2	0.8600	C8—H8B	0.9700

N1—C2	1.347 (14)	C13—C14	1.392 (15)
N1—C6	1.392 (14)	C13—C12	1.433 (16)
N1—C1	1.521 (13)	C13—H13	0.9300
C7—C4	1.540 (15)	C14—H14	0.9300
C3—C2	1.416 (15)	C12—C11	1.404 (18)
C3—C4	1.425 (14)	C12—H12	0.9300
C3—H3	0.9300	C1—H1A	0.9600
C2—H2A	0.9300	C1—H1B	0.9600
C5—C6	1.392 (16)	C1—H1C	0.9600
C5—C4	1.412 (14)	C10—C11	1.404 (17)
C5—H5	0.9300	C10—H10	0.9300
C6—H6	0.9300	C11—H11	0.9300
C9—C10	1.422 (15)		
C7—N2—C8	122.4 (9)	N2—C8—C9	113.2 (9)
C7—N2—H2	118.8	N2—C8—H8A	108.9
C8—N2—H2	118.8	C9—C8—H8A	108.9
C2—N1—C6	118.6 (11)	N2—C8—H8B	108.9
C2—N1—C1	121.3 (10)	C9—C8—H8B	108.9
C6—N1—C1	120.0 (10)	H8A—C8—H8B	107.7
O1—C7—N2	122.6 (11)	C14—C13—C12	118.6 (11)
O1—C7—C4	120.0 (10)	C14—C13—H13	120.7
N2—C7—C4	117.4 (10)	C12—C13—H13	120.7
C2—C3—C4	119.1 (10)	C13—C14—C9	123.3 (11)
C2—C3—H3	120.5	C13—C14—H14	118.4
C4—C3—H3	120.5	C9—C14—H14	118.4
N1—C2—C3	122.9 (10)	C11—C12—C13	118.9 (12)
N1—C2—H2A	118.5	C11—C12—H12	120.6
C3—C2—H2A	118.5	C13—C12—H12	120.6
C6—C5—C4	121.4 (11)	N1—C1—H1A	109.5
C6—C5—H5	119.3	N1—C1—H1B	109.5
C4—C5—H5	119.3	H1A—C1—H1B	109.5
C5—C4—C3	117.0 (11)	N1—C1—H1C	109.5
C5—C4—C7	117.3 (10)	H1A—C1—H1C	109.5
C3—C4—C7	125.7 (11)	H1B—C1—H1C	109.5
C5—C6—N1	121.0 (11)	C11—C10—C9	120.4 (12)
C5—C6—H6	119.5	C11—C10—H10	119.8
N1—C6—H6	119.5	C9—C10—H10	119.8
C10—C9—C14	117.0 (11)	C10—C11—C12	121.7 (13)
C10—C9—C8	121.2 (11)	C10—C11—H11	119.2
C14—C9—C8	121.8 (10)	C12—C11—H11	119.2
C8—N2—C7—O1	-2.8 (15)	C2—N1—C6—C5	2.6 (18)
C8—N2—C7—C4	177.7 (9)	C1—N1—C6—C5	-179.7 (13)
C6—N1—C2—C3	-2.0 (17)	C7—N2—C8—C9	93.5 (12)
C1—N1—C2—C3	-179.7 (10)	C10—C9—C8—N2	103.8 (12)
C4—C3—C2—N1	0.2 (16)	C14—C9—C8—N2	-76.9 (13)
C6—C5—C4—C3	-0.3 (19)	C12—C13—C14—C9	1.1 (17)

C6—C5—C4—C7	−178.7 (11)	C10—C9—C14—C13	−1.4 (16)
C2—C3—C4—C5	0.9 (16)	C8—C9—C14—C13	179.3 (10)
C2—C3—C4—C7	179.1 (10)	C14—C13—C12—C11	0.9 (17)
O1—C7—C4—C5	−1.4 (16)	C14—C9—C10—C11	−0.3 (18)
N2—C7—C4—C5	178.0 (10)	C8—C9—C10—C11	179.1 (12)
O1—C7—C4—C3	−179.6 (10)	C9—C10—C11—C12	2 (2)
N2—C7—C4—C3	−0.2 (15)	C13—C12—C11—C10	−3 (2)
C4—C5—C6—N1	−1 (2)		

*Hydrogen-bond geometry (Å, °)*

D—H···A	D—H	H···A	D···A	D—H···A
N2—H2···Br1	0.86	2.68	3.468 (9)	154
C1—H1 <i>A</i> ···Br1 <sup>i</sup>	0.96	3.04	3.913 (13)	152
C1—H1 <i>C</i> ···Br1 <sup>ii</sup>	0.96	3.01	3.901 (13)	154

Symmetry codes: (i)  $x-1/2, -y+1/2, -z$ ; (ii)  $x-1, y, z$ .